Comparative pore structure analysis of highly porous graphene monoliths treated at different temperatures with adsorption of N_2 at 77.4 K and of Ar at 87.3 K and 77.4 K

*Shuwen Wang, Daiki Minami, Katsumi Kaneko**

Center for Energy and Environmental Science, Shinshu University, Wakasato, Nagano, 380-8553, Japan.

*To whom correspondence should be addressed. E-mail: kkaneko@shinshu-u.ac.jp

Tel: +81-(0)26-269-5743 Fax: +81-(0)26-269-5737

Abstract: We prepared nanoporous graphene monolith of different porosity by high temperature treatment up to 2073 K in Ar. The porosity is comparatively evaluated with N_2 adsorption isotherms at 77.4 K and Ar adsorption isotherms at 87.3 K and 77.4 K. N_2 adsorption at 77.4 K shows an excess adsorption amount below 3×10^{-3} of the relative pressure which is caused by the quadrupole moment of an N_2 molecule. This effect doesn't give significant influence on the determination of the total surface area from subtracting pore effect (SPE) method, the micropore volume from Dubinin-Radushkevich (DR) method and the total pore volumes from the Gurvitch rule. However, the peak of the micropore size distribution determined by Horvath-Kawazoe (HK) method from N_2 adsorption at 77.4 K shifts to a smaller size than that from Ar adsorption at 87.3 K by 0.05 to 0.09 nm.

Keywords: Nitrogen adsorption, Argon adsorption, Nanoporous carbon, Subtracting pore effect method, Pore size distribution.

1. Introduction

Sustainable technology needs a variety of nanoporous solids which have contributed to separation, adsorption and catalysis. A more sophisticated technology has requested a better pore structure characterization. Both of high resolution transmission electron microscopy (TEM) and X-ray diffraction (XRD) can give us an explicit pore structure for crystalline porous solids, although the satisfactory application of TEM to insulative and thermally unstable crystals such as zeolites and porous coordination polymers (PCPs) is still not easy. Small angel X-ray scattering (SAXS) has contributed to evaluate the pore structure of noncrystalline porous solids, although the analysis is not simple for highly dense pore systems [1]. The TEM, XRD and SAXS methods with the expensive instruments cannot give the effective pore structure. On the contrary, N_2 adsorption at 77.4 K has offered a concise method for evaluation of the effective pore structure for molecules, being helpful to design chemical processes using the porous solids. Consequently the N_2 adsorption has been widely used for the pore structure evaluation. N_2 molecules are adsorbed in pores with physical adsorption whose attractive interaction is mainly dispersion interaction. As N_2 is a diatomic molecule, we must take into account the interaction of the quadrupole moment of N_2 with the adsorption sites on the pore wall [2, 3]. The maximum additional energy due to the electrostatic interaction between the quadrupole moment and the polar sites is only 10% order of the whole attractive interaction [4]. Nevertheless, the specific adsorption of N_2 often induces pore blocking in micropores, preventing an accurate evaluation of microporosity.

As Ar has no quadrupole moment, once many scientists have attempted to apply Ar adsorption at 77.4 K instead of N_2 adsorption at 77.4 K in order to avoid the erroneous pore characterization due to the quadrupole moment of N_2 [5-13]. Furthermore, Ar has a smaller molecular size (Lennard-Jones size parameter of Ar is 0.341 nm, whereas that of N_2 is 0.375 nm) [14], which should be a merit for characterization of small micropores. Thus, Ar adsorption at 77.4 K was expected to provide a more accurate porosity than N_2 adsorption at 77.4 K. However, 77.4 K is lower than the triple point of Ar (83.8 K) and the state of Ar at 77.4 K is not necessarily well defined; the saturation vapor pressure of supercooled liquid Ar at 77.4 K which has been widely used, gives an abnormal adsorption behavior above P/P_0 = 0.9 [15, 16]. Recently Ar adsorption at 87.3 K of boiling temperature for evaluation of microporosity has been often employed. In principle, Ar adsorption at 87.3 K should be better than N_2 adsorption at 77.4 K because of the merit mentioned above. A higher measuring temperature of Ar than N_2 by 10 K can lead to a better intrapore diffusion of Ar molecules, which should give a better pore evaluation. Surely an intensive effectiveness of Ar adsorption at 87.3 K has been shown in PCP [17, 18], zeolites [19-22] and porous carbon [23-27], and the fundamental studies have been published [28-30].

Highly porous graphene monoliths developed by these authors consist of nanographenes, which have a wide range of pores from micropores to macropores [31]. Hence this is a good model of activated carbons and the comparative pore characterization of the highly porous graphene monolith with adsorption of N_2 and Ar

can provide fundamental information on the porosity evaluation of activated carbons. In this work, we measured adsorption isotherms of the highly porous graphene monoliths heated at different temperatures for N_2 at 77.4 K and of Ar at 77.4 K and 87.3 K to discuss the effectiveness of Ar adsorption at 87.3 K.

2. Experimental

2.1. Preparation and high temperature treatment of highly porous graphene monolith

The graphene oxide was prepared from natural graphites and KOH was added to the graphene oxide suspension at the KOH/graphite weight ratio of 8. The graphene oxide monolith was prepared by the unidirectional freeze drying method. The monolith of graphene oxide and KOH mixture was heated up to 573 K in Ar to reduce the graphene oxide and then the monolith of the graphene-KOH mixture was heated to 1073 K in order to activate the graphene. The preceding X-ray photoelectron spectroscopic study showed that heating at 573 K in Ar reduced the graphene oxide sufficiently [31]. Thorough washing of the graphene activated by KOH with water provides a highly porous graphene monolith. Thus obtained graphene monolith of high surface area (named as G-O) was further heated at different temperature of 1473 K to 2073 K in Ar. The nanoporous graphene monolith treated at *T* K is named as G-*T*.

2.2. Pore structure characterization

The pore structure of nanoporous graphene monolith samples was evaluated by N_2 adsorption at 77.4 K and Ar adsorption at 87.3 K and 77.4 K by using a Micromeritics ASAP2020 surface analyzer after pre-evacuation of the sample at 473 K for 3 h. The

graphene monolith samples were pulverized to measure the adsorption isotherms. The adsorption isotherms of carbon black (Mitsubishi Chem. Co. 32B) of N_2 at 77.4 K and Ar at 87.3 K and 77.4 K were also measured as the reference data for α_s-plot analysis.

3. Results and discussion

3.1. Comparison of adsorption isotherms of N_2 at 77.4 K and Ar at 87.3 K and 77.4 K

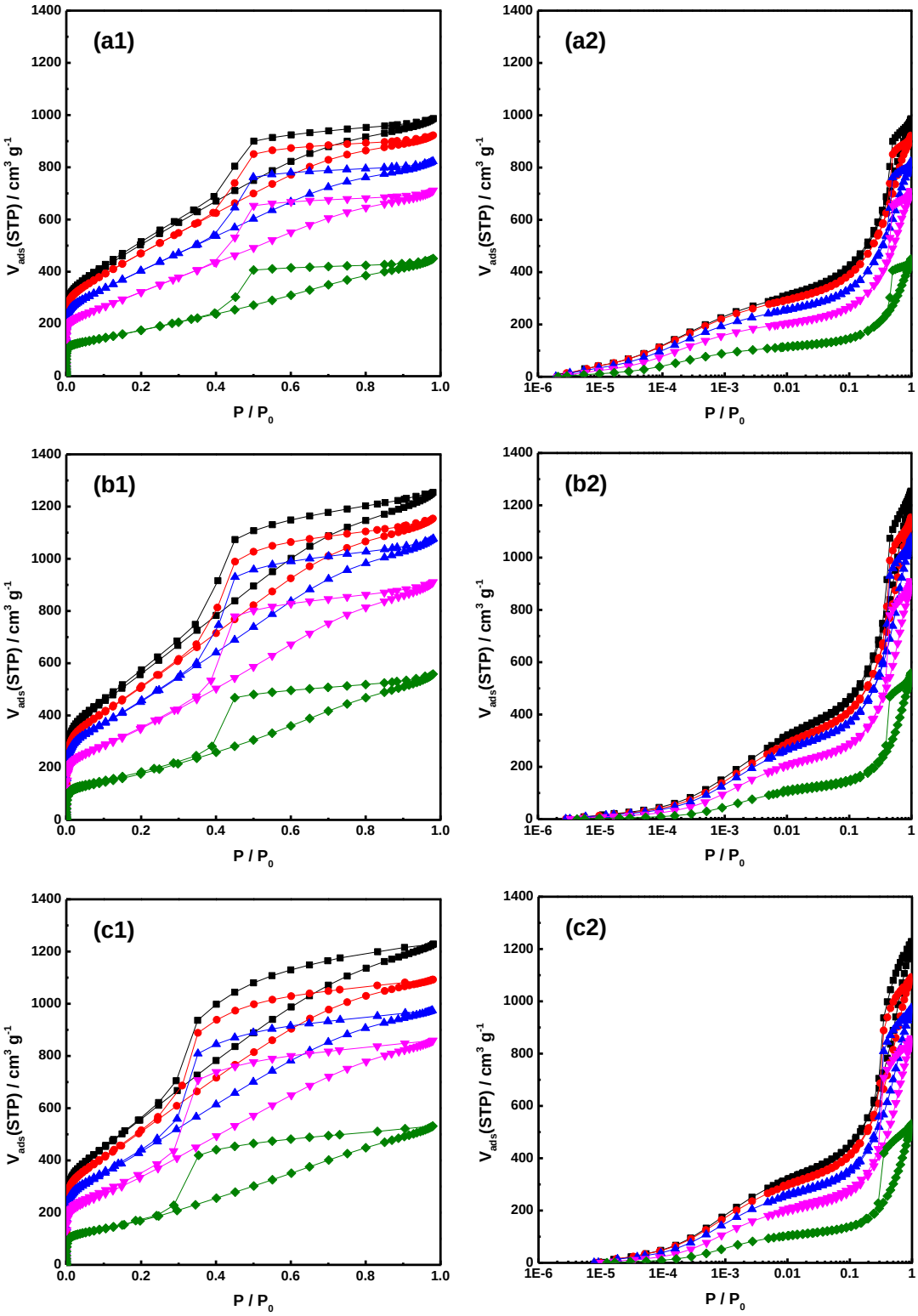

Fig. 1. Adsorption isotherms of highly porous graphenes for (a) N_2 at 77.4 K, (b) Ar at 87.3 K and (c) Ar at 77.4 K. G-O: ■, G-1473: ●, G-1673: ▲, G-1873: ▼, G-2073: ◆.

Fig. 1 shows adsorption isotherms of porous graphene samples for N_2 at 77.4 K (a), and Ar at 87.3 K (b) and 77.4 K (c). Here, all adsorption isotherms are expressed by the linear (a1, b1, and c1) and logarithmic P/P_0 (a2, b2, and c2). All adsorption isotherms with the linear P/P_0 have a sharp uptake at the initial stage and a gradual increase with P/P_0, accompanying a clear adsorption hysteresis loop of type H2, although the higher the treatment temperature, the less the adsorption amount. Consequently these nanoporous graphene samples have both of micropores and mesopores. The H2 loop was attributed to a difference in mechanism between condensation and evaporation processes occurring in pores with narrow necks and wide bodies (‘ink bottle’ pores) in the past, but now it is recognized that this model is over-simplified, because the role of network effects is not taken into account [32]. The steep uptakes in the initial stage of the linear scale adsorption isotherms correspond to gradual steps below of $P/P_0 = 4\times10^{-3}$ in the logarithmic ones. The adsorption amount of Ar at 87.3 K is evidently larger than that of N_2 at 77.4 K for each sample. This comes from the molecular area difference between Ar and N_2. The well established molecular area 0.162 nm^2 of N_2 at 77.4 K is derived from the density of liquid N_2 with the hexagonal close packing [33, 34]. In a similar way, the molecular area of Ar on the solid surface at 87.3 K is given to be 0.142 nm^2 from the liquid Ar density. The molecular area of N_2 at 77.4 K is larger than that of Ar at 87.3 K by 1.14, being close to the adsorption amount ratio of N_2 at 77.4 K against Ar at 87.3 K at $P/P_0 = 0.4$, where pore filling in the micropores finishes. Another difference between N_2 adsorption isotherms at 77.4 K and Ar adsorption isotherms at

87.3 K is on the closure point of the hysteresis loop. The hysteresis loop of N_2 closes at P/P_0 = 0.4, being well known, while the closure point of Ar is 0.35. The adsorption branch of the hysteresis loop of Ar at 77.4 K has no sharp bending as observed in Ar at 87.3 K and N_2 at 77.4 K; the closure point of Ar at 77.4 K is 0.3, being smaller than that of Ar at 87.3 K. The closure point is empirically associated with the surface tension of adsorbed layer through the tensile strength mechanism [35], although the concept cannot be supported by statistical mechanical studies. The observed closure point at the smaller P/P_0 at 77.4 K than at 87.3 K is qualitatively fit for the tensile strength mechanism. We compare the three adsorption isotherms directly, as shown in Fig. 2 for further discussion.

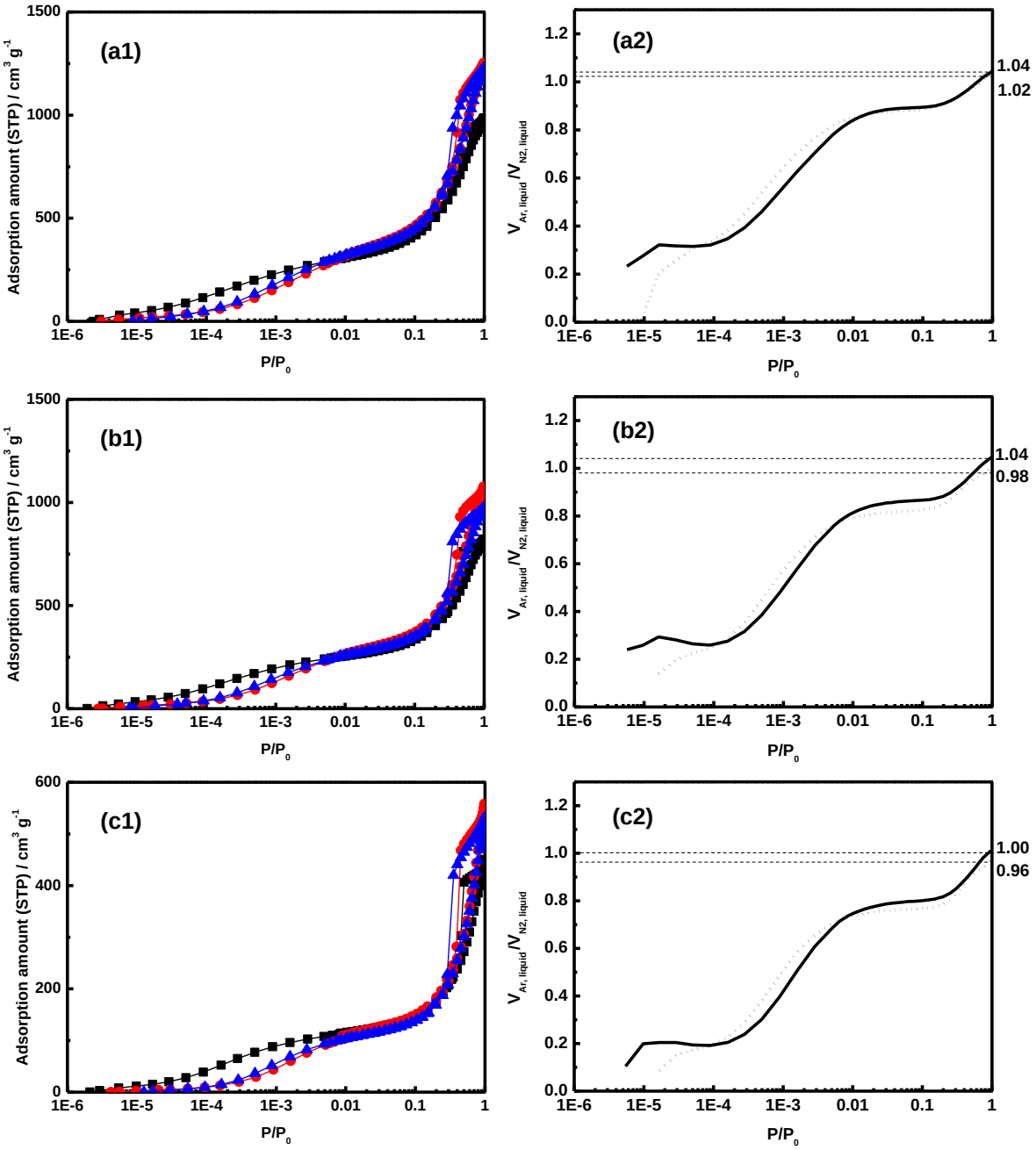

Fig. 2. Comparison of adsorption isotherms on three samples (a) G-O, (b) G-1673, (c) G-2073, and the corresponding uptake ratio of Ar to N_2 expressed by liquid volumes. N_2 at 77.4 K: ■, Ar at 87.3 K: ●, Ar at 77.4 K: ▲. $V_{Ar(87.3\ K)}$ / $V_{N2(77.4\ K)}$: Solid line, and $V_{Ar(77.4\ K)}$ / $V_{N2(77.4\ K)}$: Dotted line. Here $V_{Ar(87.3\ K)}$ is the liquid volume of Ar at 87.3 K and other notations have similar meaning. Numerical values on the right ordinate of (a2),

(b2), and (c2) mean the volume ratio at $P/P_0 = 1$.

Fig. 2 shows the logarithmic adsorption isotherms of G-O, G-1673 and G-2073 (a1, b1 and c1). Their Ar adsorption isotherms at 87.3 K and 77.4 K reduced by the saturated adsorption amount of N_2 are also shown (a2, b2, and c2). Here, the ordinates of a2, b2 and c2 are expressed by the liquid volumes of Ar at 87.3 K and 77.4 K and that of N_2 at 77.4 K using their liquid densities. Briefly speaking, Ar adsorption isotherms at 87.3 K and 77.4 K are almost similar each other below $P/P_0 = 2 \times 10^{-1}$, whereas their hysteresis loops are different from each other, which stems from the different closure point. The evident differences between N_2 and Ar adsorption isotherms are observed below $P/P_0 = \sim 10^{-2}$ and near $P/P_0 = 1$. The adsorption behavior difference near $P/P_0 = 1$ is discussed above. The adsorption amount of N_2 is much larger than that of Ar in the P/P_0 range of 10^{-5} to 3×10^{-3}. This excess adsorption of N_2 in the low pressure region is widely reported in various cases [6, 10, 26, 36, 37]. This excess adsorption N_2 comes from the additional interaction due to the quadrupole moment of the N_2 molecule. The Gurvitch rule [38] is quite useful to compare the filling state of pores by different adsorptives such as N_2 and Ar. Fig. 2(a2, b2 and c2) shows the filling ratio of Ar at 87.3 K and 77.4 K against N_2. These figures exhibit distinctly the difference of Ar adsorption between 87.3 K and 77.4 K in three regions: $P/P_0 < 10^{-4}$, $10^{-4} < P/P_0 < 10^{-2}$, and $P/P_0 > 10^{-2}$. Here we used the P_0 value of 2.93×10^4 Pa at 77.4 K being the value of the supercooled liquid Ar for construction of the adsorption isotherms at 77.4 K as usual [38]. The similar phenomenon is reported elsewhere [7]. There is no simple explanation on the

different behavior of Ar at 77.4 K from that at 87.3 K. Probably, the entrance blocking effect for adsorption in smaller micropores at 77.4 K is more marked than that at 87.3 K, giving the smaller adsorption amount than that at 87.3 K below $P/P_0 = 10^{-4}$. However, in the middle range of P/P_0, the adsorption amount at 77.4 K in the P/P_0 range is larger than that at 87.3 K, a smaller molecular area for Ar at 77.4 K than that at 87.3 K should be associated with this behavior. The blocking at the intersites between solid-like Ar clusters in mesopores at 77.4 K above $P/P_0 = 10^{-2}$ should bring about the smaller total adsorption. In the following sections, we will show the comparative analysis of the observed adsorption isotherms.

3.2 Surface area with high resolution α_s-plot analysis

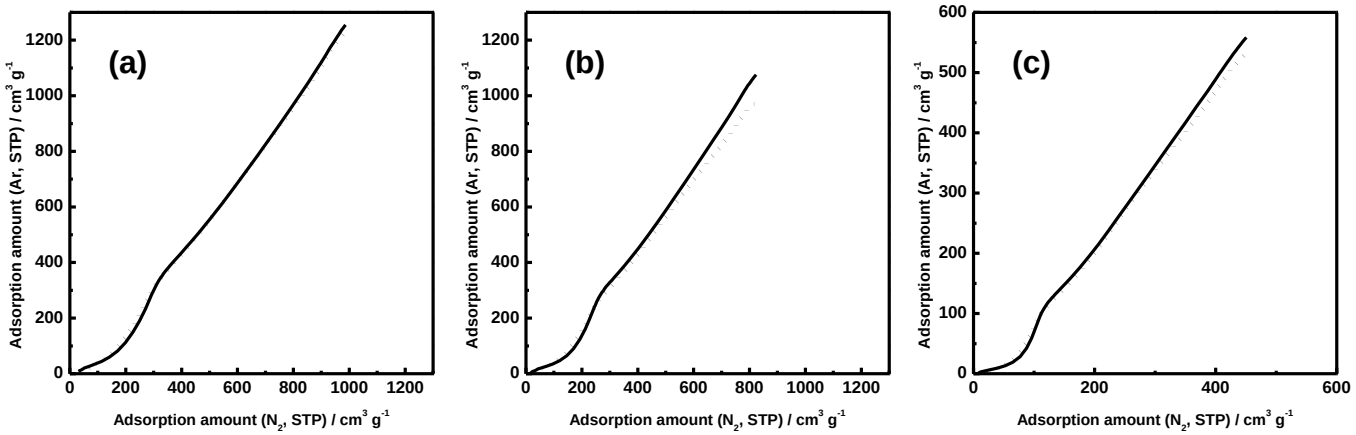

Fig. 3. Comparison plots of Ar adsorption isotherms at 87.3 K and 77.4 K against N_2 adsorption isotherms at 77.4 K for (a) G-O, (b) G-1673 and (c) G-2073. Ar at 87.3 K: Solid line, Ar at 77.4 K: Dotted line.

We have evidenced the effectiveness of the high resolution α_s-plot analysis with the subtracting pore effect SPE method for porous carbon having micropores

experimentally and theoretically in the previous studies [39, 40]. The subtracting pore effect (SPE) method can determine the monolayer capacity even in the micropores with removal of the overestimation in the monolayer capacity induced by the overlapped interaction potential effect. At first, the comparison plot will be shown in order to extract the effect by the quadrupole moment of N_2.

Fig. 3 illustrates the comparison plots of Ar adsorption isotherms at 87.3 K and 77.4 K against N_2 adsorption isotherms at 77.4 K. The complete linear plot guarantees no anomaly in the interaction of the adsorptive with the graphene sample. All comparison plots give a clear downward deviation in the initial stage of adsorption. The downward deviation indicates that the interaction between Ar and the graphene pore is weaker than that between N_2 and the graphene pore [41]. The pressure region giving the downward deviation corresponds to the monolayer formation; the interaction energy of N_2 in the monolayer with the graphene wall is larger than that of Ar due to the additional attractive energy of the quadrupole moment of N_2 with the graphene surface.

The comparison plots of Ar at 87.3 K and 77.4 K give similar results except for larger adsorption region, because Ar adsorption amount at 77.4 K is smaller than that at 87.3 K in the high pressure region, as mentioned above. Probably formation of solid-like Ar at 77.4 K should be associated with the above behavior [29].

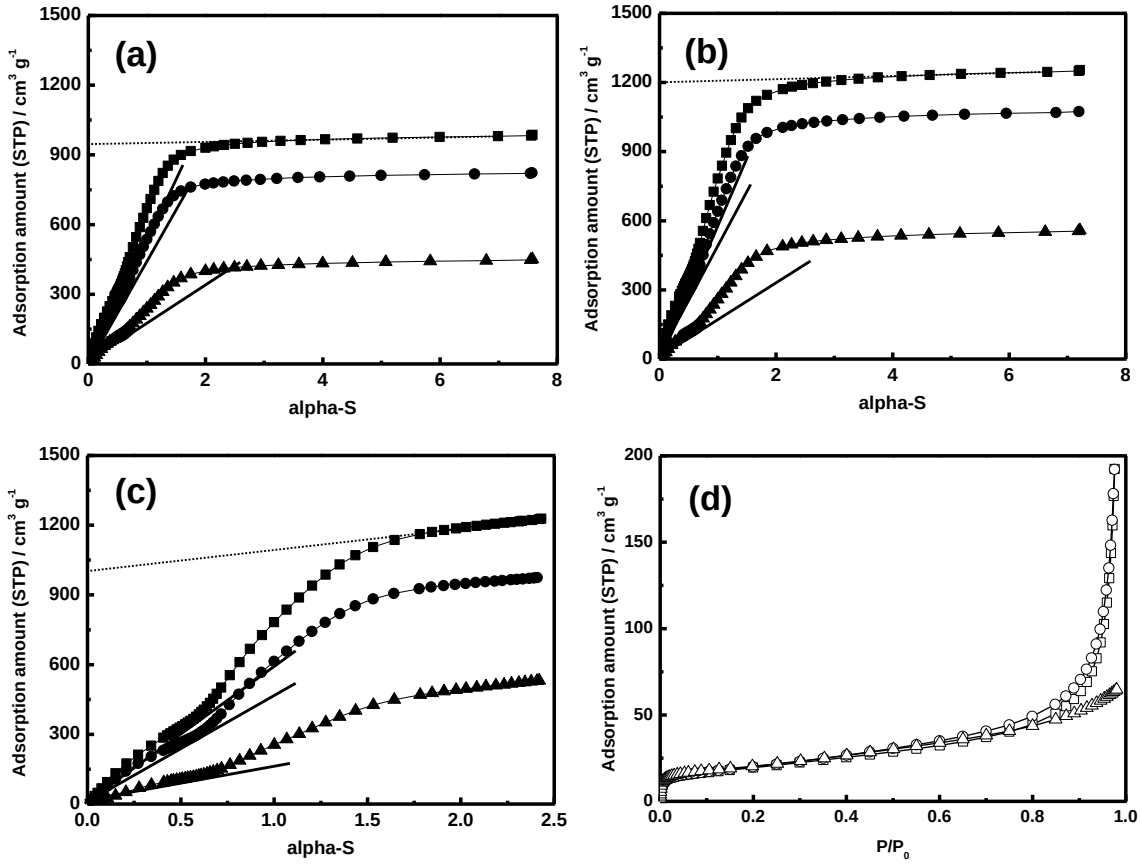

Fig. 4. The α_s-plots of adsorption isotherms of highly porous graphene monoliths for (a) N_2 at 77.4 K, (b) Ar at 87.3 K and (c) Ar at 77.4 K. G-O: ■, G-1673: ●, G-2073: ▲. Here the standard adsorption isotherms of nonporous carbon black for N_2 at 77.4 K and Ar at 87.3 K and 77.4 K are shown in (d). N_2 at 77.4 K: □, Ar at 87.3 K: ○, Ar at 77.4 K: △.

We determined the surface area of nanoporous graphene samples with the SPE method using the α_s-plot. Fig. 4 shows high resolution α_s-plots of nanoporous graphene samples for N_2 adsorption at 77.4 K and Ar adsorption at 87.3 K and 77.4 K. The standard adsorption isotherms of nonporous carbon black for N_2 at 77.4 K and Ar at 87.3 K and 77.4 K, which are used for construction of the α_s-plot, are also shown in Fig.

4. Here, Ar adsorption at 77.4 K on the carbon black does not increase in the multilayer adsorption region near $P/P_0 = 1$, which is often reported in the literatures [6, 28]. Do et al [29] indicated an undergoing phase transition of Ar from liquid-like to solid-like state in the higher pressure range at 77.4 K with GCMC simulation on the graphitized carbon black. This phase transition should give the observed slight increase near $P/P_0 = 1$, and the Ar adsorption isotherm in the higher P/P_0 region at 77.4 K is not fit for pore characterization.

The α_s-plots of N_2 at 77.4 K and Ar at 87.3 K have both of filling and condensation swings, although the condensation swing is more predominant than the filling one [39]. The presence of both swings indicates the presence of micropores of about 1 nm in width and pores of 2~3 nm in width.

Table 1

Surface areas determined from α_s-plot method and BET method by using N_2 adsorption isotherms at 77.4 K and Ar adsorption isotherms at 87.3 K and 77.4 K.

	$S_{\alpha s}$ / m^2 g^{-1}			$S_{external}$ / m^2 g^{-1}			S_{BET} / m^2 g^{-1}		
	N_2 (77.4K)	Ar (87.3K)	Ar (77.4K)	N_2 (77.4K)	Ar (87.3K)	Ar (77.4K)	N_2 (77.4K)	Ar (87.3K)	Ar (77.4K)
G-O	1560	1580	1480	30	50	--	1860	1790	1810
G-1473	1475	1460	1350	25	60	--	1730	1680	1685
G-1673	1270	1280	1160	30	60	--	1480	1400	1430
G-1873	1015	1000	900	30	50	--	1190	1120	1130
G-2073	560	510	460	30	50	--	645	565	565

The slope of the α_s-plot combining the origin and the point at $\alpha_s = 0.5$ leads to the accurate total surface area. The external surface area can be obtained from the slope of

the α_s-plot in the higher α_s region. Table 1 summarizes the surface area from the SPE method. Also the BET surface area, which is obtained from the adsorption data in the P/P_0 range of 0.05 to 0.35, is shown for comparison. The total surface area values from N_2 at 77.4 K and Ar at 87.3 K almost coincide with each other within 2%. However, the surface area from Ar at 77.4 K gives a smaller value than that from Ar at 87.3 K by about 10%. The BET surface area is much larger than the SPE surface area. This is because the routine BET analysis partially includes bilayer adsorption for evaluation of the monolayer capacity of the pore walls [39].

As to the external surface area from the SPE analysis, no excellent agreement between N_2 at 77.4 K and Ar at 87.3 K is obtained due to the very small slope of the linear plot in the higher α_s-plot region. The α_s-plot of Ar at 77.4 K cannot provide the external surface area because of narrow α_s-plot region.

3.3 Micropore volume with Dubinin-Radushkevich method

The Dubinin-Radushkevich (DR) plot has been widely used to evaluate the micropore volume of porous carbons [42-44]. The DR plots give a similar linearity in the lower pressure range for all samples. Fig. 5 shows the DR plots of N_2 at 77.4 K and Ar at 87.3 K and 77.4 K for G-1673 as an example. As the extrapolation of the linear plot in the low pressure region leads to the micropore volume. Table 2 lists the micropore volume determined by the DR plot of the adsorption isotherm of N_2 at 77.4 K and Ar at 87.3 K and 77.4 K.

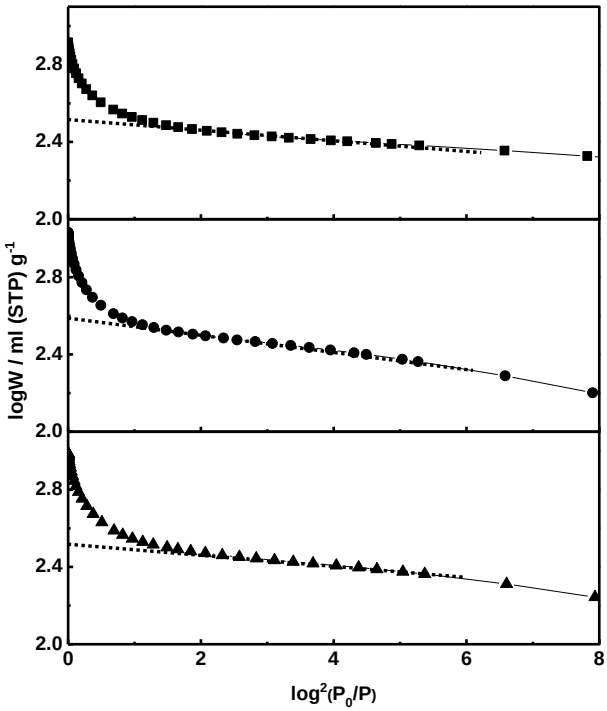

Fig.5. DR plots for N_2 adsorption isotherms at 77.4 K and Ar adsorption isotherm at 87.3 K and 77.4 K on G-1673. N_2 at 77.4 K: ■, Ar at 87.3 K: ●, Ar at 77.4 K: ▲.

Table 2

Micropore volume and total pore volume.

	V_{micro} / cm^3 g^{-1}			V_{total} / cm^3 g^{-1}		
	N_2 (77.4K)	Ar (87.3K)	Ar (77.4K)	N_2 (77.4K)	Ar (87.3K)	Ar (77.4K)
G-O	0.59	0.58	0.56	1.53	1.59	1.56
G-1473	0.56	0.53	0.50	1.43	1.46	1.38
G-1673	0.48	0.48	0.43	1.29	1.34	1.26
G-1873	0.38	0.36	0.34	1.11	1.15	1.08
G-2073	0.21	0.18	0.17	0.70	0.70	0.67

The micropore volume from Ar at 87.3 K agrees well with that from N_2 at 77.4 K, whereas the micropore volume from Ar at 77.4 K is slightly smaller than that from N_2 at 77.4 K. Consequently, the availability of N_2 adsorption at 77.4 K for evaluation of micropores is almost similar to that of Ar adsorption at 87.3 K. The total pore volumes

determined from adsorption amount at $P/P_0 = 0.98$ from N_2 and Ar adsorption isotherms are also shown in Table 2. The total pore volume from N_2 at 77.4 K almost agrees with that from Ar at 87.3 K. Even the total pore volume from Ar at 77.4 K is close to that from Ar at 87.3 K.

3.4. Pore size distribution from Horvath-Kawazoe method

As the filling pressure of N_2 at 77.4 K is smaller than that of Ar at 87.3 K due to the presence of the quadrupole moment of N_2, the micropore size distribution should depend on the adsorptive. Here we applied the classical Horvath-Kawazoe (HK) method which gives a brief feature of the pore size distribution [45, 46].

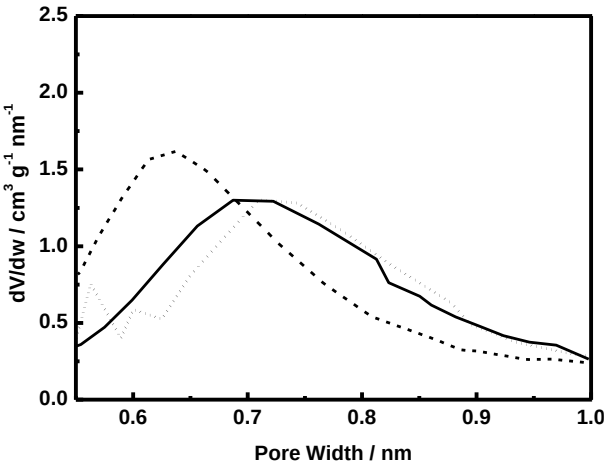

Fig. 6. Pore size distributions of highly porous graphene monoliths (G-1673) from adsorption of N_2 at 77.4 K and of Ar at 87.3 K and 77.4 K. N_2 at 77.4 K: Dashed line, Ar at 87.3 K: Solid line, and Ar at 77.4 K: Dotted line.

Fig. 6 shows the micropore size distributions of G-1673 obtained by the HK method from adsorption isotherms with adsorptive of N_2 at 77.4 K and Ar at 87.3 K and 77.4 K. All pore size distribution curves have a broad peak at the different position. The N_2

adsorption isotherm at 77.4 K gives the peak at the smallest position (around 0.6 nm) of three pore size distributions. The peaks of the pore size distributions from Ar adsorption isotherms at 87.3 K and 77.4 K are situated around 0.7 nm; the peak from Ar at 77.4 K slightly shifts to a larger value than that from Ar at 87.3 K because of the delayed filling of Ar at 77.4 K. For all measured samples, the peak positions from Ar adsorption isotherms at 87.3 K are evidently larger than those from N_2 adsorptions at 77.4 K but slightly smaller than those from Ar adsorptions at 77.4 K, as shown in Table 3. Thus, the effect of the enhanced filling of N_2 due to the quadrupole moment cannot be neglected for evaluation of the pore size distribution; the pore size by N_2 adsorption is markedly underestimated. Consequently, we must pay attention to evaluation of the micropore size with N_2 adsorption at 77 K.

Table 3

Peak position of pore size distribution of highly porous graphene monoliths from adsorption isotherms of N_2 at 77.4 K and Ar at 87.3 K and 77.4 K.

	Peak position / nm		
	N_2 (77.4K)	Ar (87.3K)	Ar (77.4K)
G-O	0.58	0.63	0.64
G-1473	0.62	0.71	0.72
G-1673	0.63	0.71	0.73
G-1873	0.64	0.71	0.73
G-2073	0.64	0.72	0.73

4. Conclusions

In this work we have discussed the availability of Ar adsorption isotherm at 87.3 K and 77.4 K on determination of surface area, micropore volume, total pore volume and

micropore size distribution. The total surface area determined from N_2 at 77.4 K and Ar at 87.3 K with SPE method shows good consistency with each other, while that from Ar at 77.4 K gives a smaller value than that from Ar adsorption isotherm at 87.3 K by about 10%. Ar adsorption at 77.4 K is not appropriate for evaluation of the surface area of the graphene-based samples. The micropore volume determined from the DR plot method by using N_2 at 77.4 K and Ar at 87.3 K agrees well with each other, while that from Ar at 77.4 K shows slightly a smaller value. The total pore volumes obtained from the Gurvitch rule by using three different isotherms are also similar to each other. The adsorption at 77.4 K is also less applicable for evaluation of the micropore value. The peak of micropore size distribution from HK method with N_2 at 77.4 K shifts to a smaller size than that with Ar adsorption at 87.3 K by 0.05-0.09 nm, which is ascribed to the quadrupole moment-associated filling of N_2. On the other hand, Ar adsorption at 77.4 K provides slightly larger pore size than Ar adsorption at 87.3 K due to the delayed filling. Thus, the Ar adsorption at 87.3 K is the most preferable to evaluate the micropore structure of the nanoporous graphenes. Then Ar at 87.3 K is recommended to determine the micropore size distribution.

Acknowledgements

D. M. and S. W. were supported by JST CREST “Creation of Innovative Functional Materials with Advanced Properties by Hyper-nano-space Design” and Concert-Japan project: Efficient Energy Storage and Distribution, JST, respectively. This work was partially supported by Grant-in-Aid for Scientific Research (A) (No. 24241038) by

JSPS.

References

[1] O. Glatter, O. Kratky. Small Angle X-ray Scattering. Academic Press, London, 1982, pp. 136-138.

[2] A.D. Buckingham, R.L. Disch, D.A. Dunmur. J. Am. Chem. Soc. 90 (1968) 3104-3107.

[3] A.V. Kiselev. J. Colloid Interface Sci. 28 (1968) 430-442.

[4] G.C. Maitland, M. Rigby, E.B. Smith, W.A. Wakeham. Intermolecular Forces: Their Origin and determination. Clarendon Press, Oxford, 1987, pp. 21.

[5] J.D. Carruthers, D.A Payne, K.S.W. Sing, L.J. Stryker. J. Colloid Interface Sci. 36 (1971) 205-216.

[6] D.A. Payne, K.S.W. Sing, D.H. Turk. J. Colloid Interface Sci. 43 (1973) 287-293.

[7] M.A. Bañares-Muñoz, L.V. Flores González, J.M. Martín Llorenta. Carbon 25 (1987) 603-608.

[8] J. Fernandez-Colinas, R. Denoyel, Y. Grillet, F. Rouquerol, J. Rouquerol. Langmuir 5 (1989) 1205-1210.

[9] M.J. Sellés-Pérez, J.M. Martín-Martínez. Carbon 30 (1992) 41-46.

[10] P.I. Ravikovitch , D.Wei , W.T. Chueh, G.L. Haller, A.V. Neimark. J. Phys. Chem. B 101 (1997) 3671-3679.

[11] M. Kruk, M. Jaroniec. J. Phys. Chem. B 106 (2002) 4732-4739.

[12] I. Nowak, M. Jaroniec. Appl. Surf. Sci. 253 (2007) 5676-5681.

[13] J. Choma, J. Górka, M. Jaroniec. Micropor. Mesopor. Mat. 2008 (112) 573-579.

[14] J. Pikunic, P. Llewellyn, R. Pellenq, K.E. Gubbins. Langmuir 21 (2005) 4431-4440.

[15] A.V. Neimark, P.I. Ravikovitch, M. Grün, F. Schüth, K.K. Unger. J. Colloid Interface Sci. 207 (1998) 159-169.

[16] M. Thommes. J. Phys. Chem. B 104 (2000) 7932-7943.

[17] D. Lässig, J. Lincke, J. Moellmer, C. Reichenbach, A. Moeller, R. Gläser, et al. Angew. Chem. Int. Ed. 2011, 50, 10344-10348.

[18] M. Thommes, J. Morell, K.A. Cychosz, M. Fröba. Langmuir 29 (2013) 14893-14902.

[19] A.V. Neimark, P.I. Ravikovitch, M. Grün, F. Schüth, K.K. Unger. J. Colloid Interface Sci. 207 (1998) 159-169.

[20] M. Kruk, M. Jaroniec. Chem. Mater. 12 (2000) 222-230.

[21] M. Kruk, M. Jaroniec. Micropor. Mesopor. Mat. 44-45 (2001) 725-732.

[22] O. Šolcová, L. Matějová, P. Topka, Z. Musilová, P. Schneider. J. Porous Mat. 18 (2011) 557-565.

[23] T.X. Nguyen, S.K. Bhatia. Carbon 43 (2005) 775-785.

[24] T.X. Nguyen, S.K. Bhatia. Carbon 44 (2006) 646-652.

[25] J.C. Palmer, J.D. Moore, J.K. Brennan, K.E. Gubbins. Adsorption 17 (2011) 189-199.

[26] J. Silvestre-Albero, A. Silvestre-Albero, F. Rodríguez-Reinoso, M. Thommes.

Carbon 50 (2012) 3128-3133.

[27] S. Rols, M.R. Johnson, P. Zeppenfeld, M. Bienfait, O.E. Vilches, J. Schneble. Phys. Rev. B 71 (2005) 155411-155418.

[28] L. Gardner, M. Kruk, M. Jaroniec. J. Phys. Chem. B 105 (2001) 12516-12523.

[29] D.D. Do, H.D. Do, D. Nicholson. Adsorpt. Sci. Technol. 25 (2007) 347-363.

[30] A. Silvestre-Albero, J. Silvestre-Albero, M. Martínez-Escandell, R. Futamura, T. Itoh, K. Kaneko, F. Rodríguez-Reinoso. Carbon 66 (2014) 699-704.

[31] S. Wang, F. Tristan, D. Minami, T. Fujimori, R. Cruz-Silva, et al. Carbon 76 (2014) 220-231.

[32] K.S.W. Sing, D.H. Everett, R.A.W. Haul, L. Moscou, R.A. Pierotti, J. Rouquerol, T. Siemieniewska. Pure & Appl Chem. 57(1985) 603-619.

[33] J.K. Kjems, L. Passell, H. Taub, J.G. Dash. Phys. Rev. Lett. 32 (1974) 724-727.

[34] J. Rouquerol, S. Partyka, F. Rouquerol. J. Chem. Soc., Faraday Trans. 1, 73 (1977) 306-314.

[35] C.G.V. Burgess, D.H. Everett, S. Nuttall. Pure Appl. Chem. 61 (1989) 1845-1852.

[36] J. Jagiello, M. Thommes. Carbon 42 (2004) 1227-1232.

[37] E.A. Ustinova, D.D. Do. Carbon 43 (2005) 2463-2473.

[38] S.J. Gregg, K.S.W. Sing. Adsorption, Surface Area and Porosity, 2nd ed, Academic Press, New York, 1982, pp. 74, 113.

[39] N. Setoyama, T. Suzuki, K. Kaneko. Carbon 36 (1998) 1459-1467.

[40] K. Kaneko, C. Ishii, M. Ruike, H. Kuwabara. Carbon 30 (1992) 1075-1088.

[41] M. Jaroniec, K. Kaneko. Langmuir 13 (1997) 6589-6596.

[42] M.M. Dubinin. Carbon 27 (1989) 457-467.

[43] M.T. González, M. Molina-Sabio, F. Rodríguez-Reinoso. Carbon 32 (1994) 1407-1413.

[44] C.M. Yang, K. Kaneko. Carbon 39 (2001) 1075-1082.

[45] G. Horvath, K. Kawazoe. J. Chem. Eng. Jpn. 16 (1983) 470-475.

[46] L.S. Cheng, R.T. Yang. Chem. Eng. Sci. 49 (1994) 2599-2609.

Graphitical abstract

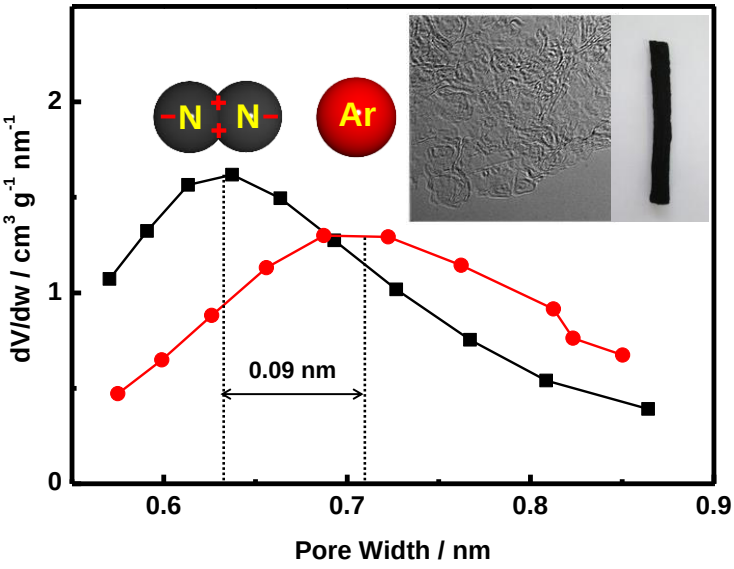

Highlights

Ar adsorption at 87.3 K gives the most reliable microporosity.

BET analysis overestimates the surface area by more than 10%.

Microporosity from Ar adsorption at 77.4 K is different from that from Ar adsorption at 87.3 K.

N_2 adsorption at 77.4 K leads to a smaller pore size due to quadrupole moment effect of N_2.